Available online at www.sciencedirect.com
SCIENCE DIRECT
International Journal of Mass Spectrometry 245 (2005) 53–60
International Journal of Mass Spectrometry
www.elsevier.com/locate/ijms

Loss of water and hydrogen atom from the *n*-propanol molecular cation: A theoretical study

Joong Chul Choe *

Department of Chemistry, University of Suwon, P.O. Box 77, Suwon 440-600, Republic of Korea

Received 3 May 2005; received in revised form 29 June 2005; accepted 1 July 2005
Available online 11 August 2005

Abstract

The unimolecular dissociation of *n*-propanol molecular cation (**1**) has been investigated theoretically. Density functional theory (DFT) molecular orbital calculations have been performed at the UB3LYP/aug-cc-pVQZ//UB3LYP/6-31 + G(d) level to obtain pathways for water and hydrogen atom loss from **1**. On the basis of the DFT results, the rate-energy dependences have been calculated for water and hydrogen atom loss from various deuterated analogues of **1** by Rice–Ramsperger–Kassel–Marcus modeling. The large kinetic deuterium isotope effects on the metastable water and hydrogen atom loss reported previously are rationalized from the obtained rate-energy dependences.

Keywords: *n*-Propanol ion; Isotope effect; Metastable ion; DFT calculation; RRKM calculation

1. Introduction

The dissociation of *n*-propanol molecular cation (**1**) has been studied by various experimental and theoretical means [1–12]. It is well known that the low energy (metastable) *n*-propanol ion dissociates mainly by loss of water. Deuterium labeling studies [5,7–9,11] revealed that the water product contains exclusively the OH group and the γ-hydrogen atoms. Theoretical calculations [4,5,10,12] suggest that the cyclopropane cation is produced by loss of water via a distonic ion, $^{\bullet}CH_2CH_2CH_2OH_2^+$, formed by 1,4-H shift and an ion–molecule complex, c-$C_3H_6^{\bullet+}\cdots H_2O$. The other competing channel is loss of hydrogen atom, minor in the metastable dissociation of **1**. The general consensus is that the H loss is also highly regiospecific. Only one of the α-hydrogen atoms is lost to produce protonated propanal.

Ab initio molecular orbital studies have been carried out by several groups. Booze and Baer [10] reported theoretical pathways for both the H_2O and H loss channels, while the others [4,5,12] did only the former. Their energy data obtained by the MP2 calculations, however, do not agree with the experimental ones. The calculated barrier for the H_2O loss is higher than that for the H loss, while the reverse is true in experimental observations [7–9,11]. This demands a better theoretical estimate close to the experimental results. A more interesting problem remained unresolved for the dissociation of **1** is extremely large deuterium isotope effect in the H loss. Bowen et al. [9] have reported a kinetic isotope effect of approximately 500:1 on hydrogen atom loss from metastable **1** without reasonable interpretation of its precise origin. Also, large is the reported isotope effect on the water loss, ∼54:1.

In this work, we try to find out the origin of the extraordinarily large isotope effects. The results of density functional theory (DFT) calculations to obtain pathways for the H_2O and H loss are reported, which are used for Rice–Ramsperger–Kassel–Marcus [13] (RRKM) model calculations to account for the isotope effects.

2. Computational methods

2.1. Quantum chemical calculation

Molecular orbital calculations were performed with the Gaussian 03 suite of programs [14]. Geometry optimizations

* Tel.: +82 31 220 2150; fax: +82 31 222 9385.
E-mail address: jcchoe@suwon.ac.kr.

1387-3806/$ – see front matter © 2005 Elsevier B.V. All rights reserved.
doi:10.1016/j.ijms.2005.07.005

for the molecular ions, intermediates, and fragments were carried out at the unrestricted B3LYP [15] (UB3LYP) density functional levels of theory [16] using the 6-31 + G(d) basis set. Transition state (TS) geometries connecting the stable structures were searched at the same level. All the TS geometries found were checked by calculating the intrinsic reaction coordinates. The harmonic vibrational frequencies and the zero-point energies (ZPEs) for the optimized structures were calculated at the UB3LYP/6-31 + G(d) level and used without scaling. For better accuracy, the total energies were calculated at the UB3LYP/aug-cc-pVQZ level with the geometries optimized at the UB3LYP/6-31 + G(d) level. For selected species, energy calculations at the UCCSD(T) [17]/aug-cc-pVDZ level were carried out. In all the reported energy data, the ZPEs are included.

2.2. RRKM calculation of rate constants

The RRKM expression [13] with tunneling was used to calculate the rate-energy dependences:

$$k(E) = \frac{\sigma}{h\rho(E)} \int_{-E_0}^{E-E_0} \kappa(\varepsilon)\rho^{\neq}(E - E_0 - \varepsilon)\mathrm{d}\varepsilon, \quad (1)$$

where E and E_0 are the reactant internal energy and the activation energy for the reaction, respectively, ε the energy in the one-dimensional reaction coordinate, ρ and $\rho^{\neq}$ the densities of states of the reactant and the transition state, respectively, σ the reaction path degeneracy, and κ is the tunneling probability calculated by treating the barrier along the reaction coordinate as the Eckart potential [18].

3. Results and discussion

3.1. DFT calculations

The recent ab initio calculations [10,12,19] agree that the optimized structure of the most stable *n*-propanol ion is quite different from its neutral structure. Elongation of C_α–C_β bonds upon ionization is the characteristics of aliphatic alcohols having two to four carbon atoms [12,19,20]. The C_α–C_β bond of **1** is elongated also in the present DFT calculation. The calculated C_α–C_β bond length of a *gauche* form of **1** (**1g**) (1.847 Å, see Fig. 1), similar to those of the previous MP2/6-31G(d, p) (1.993 Å) [10] and MP2(fc)/6-31G(d) calculations (1.759 Å) [12], is longer than that of neutral *n*-propanol (1.524 Å). There exist three stable **1** conformations formed by internal rotation about the C_α–O bond, two *gauch*e forms (**1g**, **1g′**) and one *trans* form (**1t**). Their energies are almost the same. The torsional barriers connecting the three conformations are in the range 6–10 kJ mol^{-1} (Fig. 2).

Each conformation of **1** can lose each hydrogen atom of the two α-H atoms. The numbering of the α-H atoms is shown in Fig. 1 or Fig. 2. As an example, the pathway for H1 loss from **1g** is shown in Fig. 1 together with optimized geometries. Consequently, H loss occurs via six different transition states to produce six conformations of protonated propanal as shown in Fig. 2. Two pairs out of the six conformations are optical isomers. One is produced by H1 loss from **1t** and **1g′**, and the other by H2 loss from **1g** and **1t**. The six H loss barriers lie 91–95 kJ mol^{-1} above **1g**. The reverse barriers for production of the six protonated propanal conformations are small, 2–5 kJ mol^{-1}.

As shown in Fig. 1, water loss from **1** is initialized from **1g** by 1,4 shift of one hydrogen atom of the γ-H atoms. Through two distonic ions $^{\bullet}CH_2CH_2CH_2OH_2^+$ (**2a** and **2b**) of *gauche* conformations, an ion-molecule complex, c-$C_3H_6^{\bullet+}\cdots H_2O$ (**3a**), is formed. **3a** can be considered as another distonic ion of *trans* conformation. After rearrangement of the H_2O moiety, it further isomerizes to another ion-molecule complex having C_s symmetry, c-$C_3H_6^{\bullet+}\cdots H_2O$ (**3b**). **3b** can lose water without a reverse barrier to produce the cyclopropane cation. The lowest potential energy diagram for the H_2O and H loss is shown in Fig. 3.

One can consider another pathway to lose H_2O not via isomerizations but directly from the molecular ion. We tried but failed to locate such a transition state. Moreover, the previous experiments [8,9] showed that the kinetic energy release in the H_2O loss is small (1.3–1.4 kJ mol^{-1} measured at half-height) and the metastable peak is of a simple Gaussian shape. This indicates that the H_2O loss occurs without a considerable reverse barrier, agreeing with the present pathway via ion–molecule complexes. If the H_2O loss occurred directly with a considerable reverse barrier, the kinetic energy release would be much larger.

The mechanistic picture of the obtained pathways is very similar to the MP2 result by Booze and Baer [10], even though the detailed energy data are different significantly (Table 1). Some experimental energy data are also listed in Table 1. As pointed out by Booze and Baer, the uncertainty of the experimental energies is considerable. Moreover, reliable experimental heat of formation of **1** has not been reported. We used the value of 703 kJ mol^{-1} for it, derived by Booze and Baer [11] from RRKM model calculations to fit their photoelectron–photoion (PEPICO) data, to estimate the relative experimental energies. The present DFT result shows an improvement over the previous MP2 result. The calculated H loss barrier is higher than the barrier (**TS12**) to lose H_2O, agreeing with the experimental observations, even though the quantitative agreement is not satisfactory. Since these barriers are important in the RRKM model calculations, we calculated their energies at a higher level, the UCCSD(T)/aug-cc-pVDZ level, with the geometries optimized at the UB3LYP/6-31 + G(d) level. The resultant activation barriers for the H_2O and H loss are 70.5 and 72.5 kJ mol^{-1}, respectively, which still disagree with the experimental ones of 92 and 99 kJ mol^{-1}, respectively.

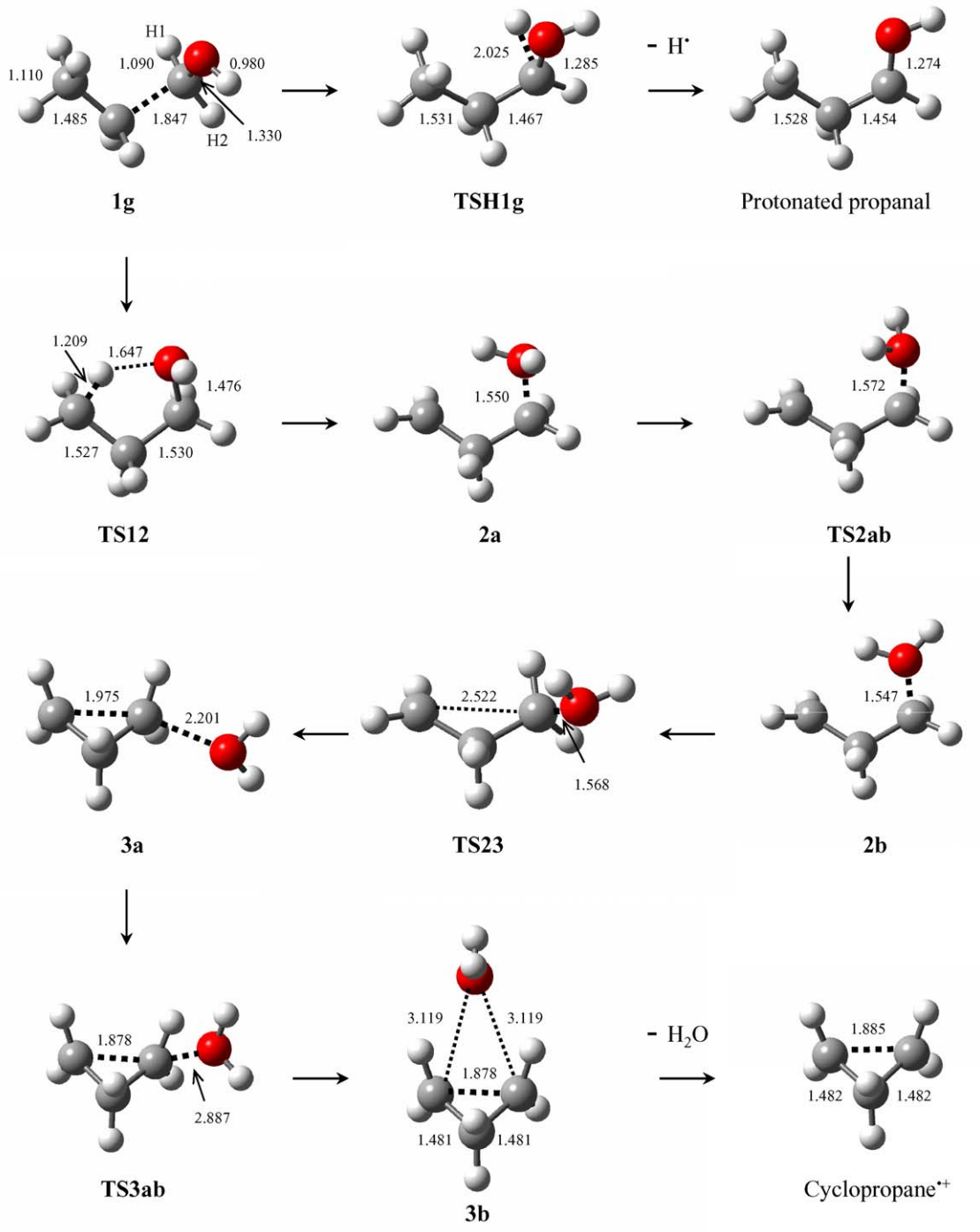

Fig. 1. The pathways for H_2O and H loss from *n*-propanol ion obtained by UB3LYP/aug-cc-pVQZ//UB3LYP/6-31 + G(d) DFT calculations. One pathway of six for the H loss, H1 loss from **1g**, is shown. The numbers are the bond lengths in Å.

3.2. RRKM model calculations

Bowen et al. [8,9] studied twice the unimolecular dissociation of metastable **1** by means of deuterium labeling. In the later study [9], they reported the deuterium isotope effects on H and H_2O loss as ∼500:1 and ∼54:1, respectively. The intramolecular k_H/k_D isotope effect is estimated from relative abundances of the metastable peaks by loss of H and D from $CD_3CH_2CHDOH^{\bullet+}$. The intermolecular k_{H_2O}:k_{HOD} isotope effect is estimated from the experiments on $CH_3CH_2CH_2OH^{\bullet+}$ and $CD_3CH_2CH_2OH^{\bullet+}$. To find out the origin of these large isotope effects, we carried out the dissociation rate calculations by RRKM modeling.

Since H loss can occur via the six barriers from three conformations of **1**, densities of all these reactant and TS states were considered [13] in the calculation of the H loss rate con-

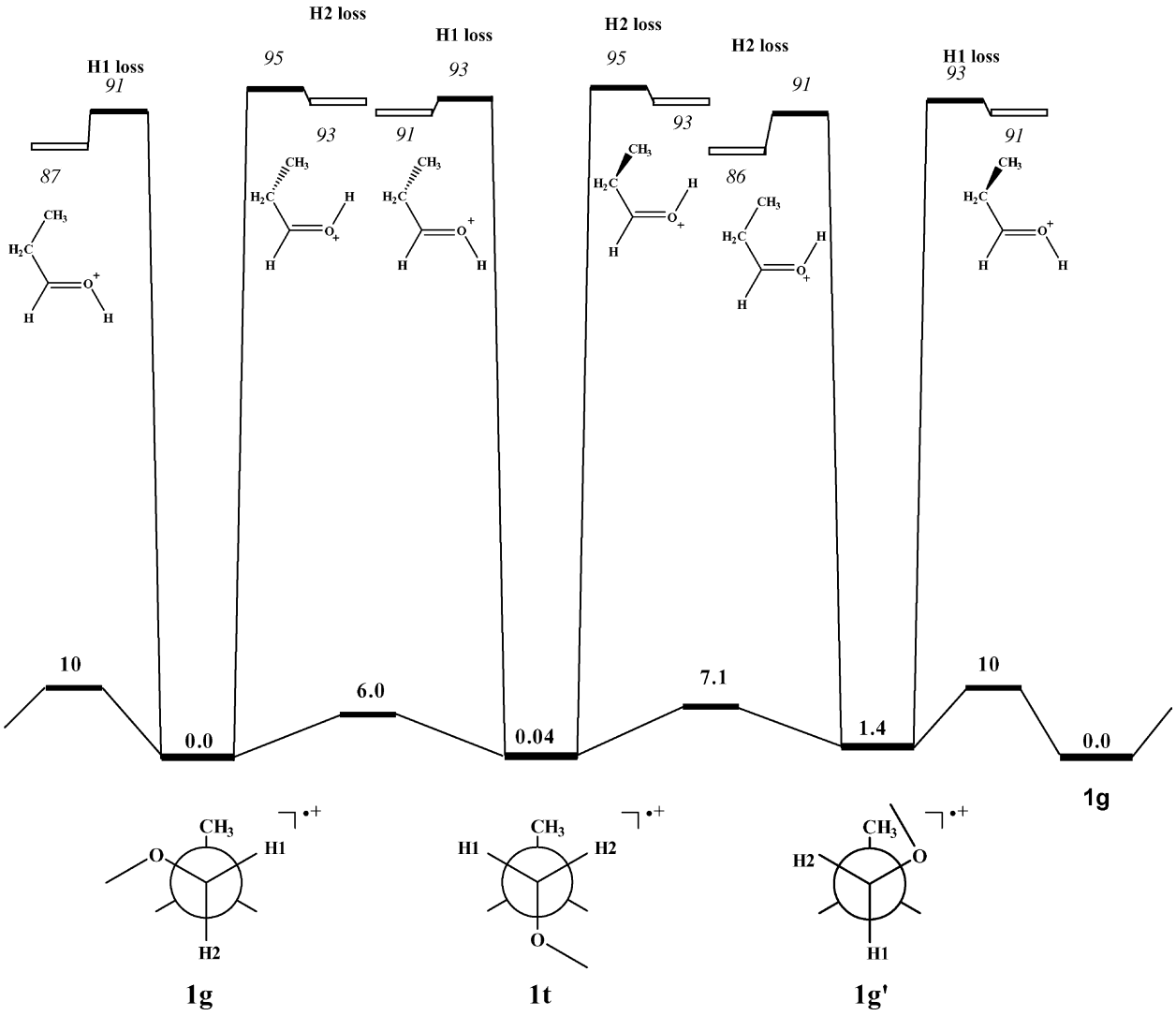

Fig. 2. Potential energy diagram for H loss from *n*-propanol ion derived from the UB3LYP/aug-cc-pVQZ//UB3LYP/6-31 + G(d) calculations. The italic numbers are the relative energies in kJ mol^{-1}.

stant, k_H. Since the barrier of the isomerization **1g** → **2a** is the highest in the pathway for H_2O loss (Fig. 3), the isomerization is the rate-determining step. This agrees with the previous experimental and theoretical results. All the contributions of three **1** conformations were considered also in the calculation of the isomerization rate constant, k_{isom}, essentially the same as the H_2O loss rate constant, k_{H_2O}. Since both these two reactions involve H rearrangement, the RRKM formula (Eq. (1)) with tunneling was used in the rate calculations. However, the $k_H(E)$ and $k_{isom}(E)$ for $CH_3CH_2CH_2OH^{\bullet+}$ calculated using the corresponding energy barriers obtained in the present DFT calculations largely deviated from the results of the PEPICO [11] and metastable ion [8,9] studies. This is because RRKM calculations are very sensitive to activation barriers. Hence, we used the experimentally estimated barriers, 92 and 99 kJ mol^{-1} for the H_2O and H loss [11], respectively, in the rate calculations. Namely, the **1g** → **2a** isomerization barrier was adjusted by adding 19 kJ mol^{-1} to the DFT results, and the H loss barriers by adding 8 kJ mol^{-1} in all the RRKM calculations described below. The vibrational frequencies were used as obtained. The resultant $k_{isom}(E)$ for $CH_3CH_2CH_2OH^{\bullet+}$ agreed well with that of Booze and Baer [11] obtained by fitting the PEPICO experimental data. The calculated $k_H(E)$ agreed well at low energy with, but somewhat deviated at high energy from the $k_H(E)$ of Booze and Baer. The accuracy of the present rate-energy dependences is enough for the purpose of understanding the isotope effects in question.

3.2.1. Intramolecular isotope effect on the hydrogen atom loss

Fig. 4a shows the rate-energy dependences of the H and D loss, $k_H(E)$ and $k_D(E)$, respectively, from $CD_3CH_2CHDOH^{\bullet+}$ together with that of HOD loss, $k_{HOD}(E)$. For each of the H and D loss, six TS and six precursor configurations are distinguishable. All the chan-

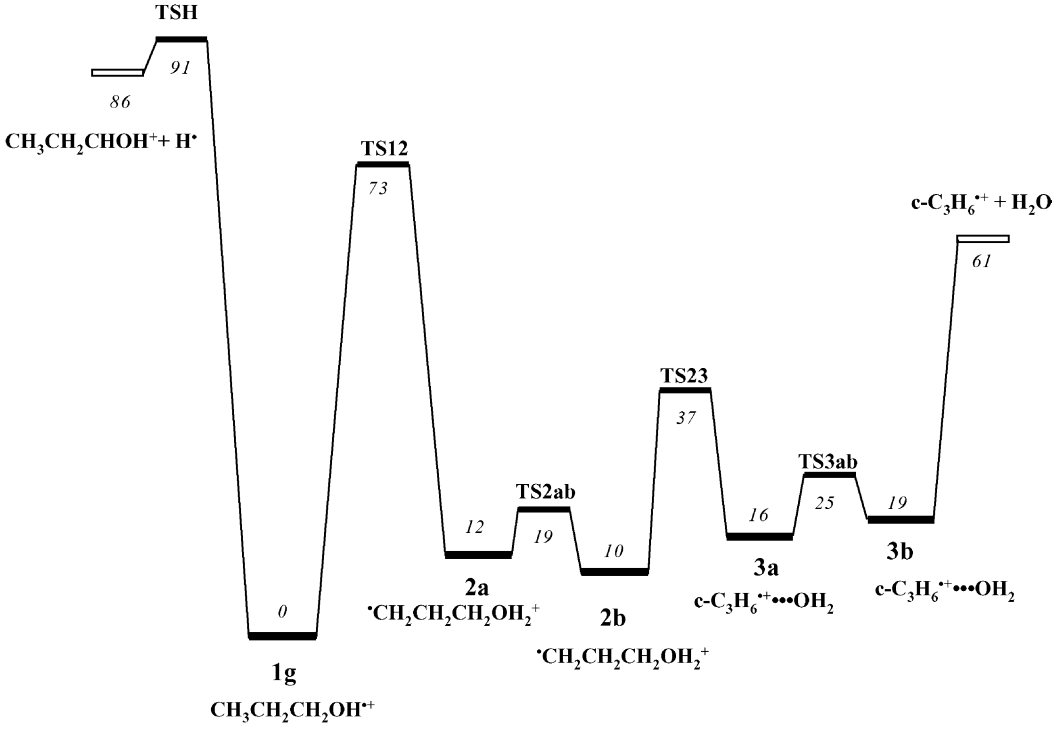

Fig. 3. Potential energy diagram for H_2O and H loss from *n*-propanol ion derived from the UB3LYP/aug-cc-pVQZ//UB3LYP/6-31 + G(d) calculations. The H loss pathway is the lowest energy one. The italic numbers are the relative energies in kJ mol^{-1}.

nels involving these were considered in the rate calculations. Some activation barriers used in the RRKM calculations are listed in Table 2. The difference in kinetics of the H and D loss arises mainly from different ZPEs of the corresponding transition states. For example, the calculated ZPE of the TS for H1 loss from a **1g** form, $CD_3CH_2CH(1)D(2)OH^{\bullet+}$, is 225.6 kJ mol^{-1}, while that for D2 loss 234.4 kJ mol^{-1}. The vibrational frequency of a C_α–D2 stretching of the TS for H1 loss is calculated as 2365 cm^{-1}, while that for the corresponding C_α–H1 stretching of the TS for D2 loss as 3148 cm^{-1}.

It is to be noted that with tandem mass spectrometric method, employed by Bowen et al. to investigate metastable ion dissociation, one cannot observe dissociation of ions with well-defined internal energy. In general, product ions from a metastable precursor ion are observed when the dissociation occurs with total dissociation rate constant (k_{tot}) of 10^4–10^6 s^{-1} [22]. Therefore, the ions undergoing metastable dissociation actually have a range of internal energy, so called metastable window, dependent on the slope of $k_{tot}(E)$. The metastable window (95–111 kJ mol^{-1}), corresponding to k_{tot} ($= k_H + k_D + k_{HOD}$) of 10^4–10^6 s^{-1}, is marked in Fig. 4 for dissociation of $CD_3CH_2CHDOH^{\bullet+}$. The k_H/k_D ratio calculated from the RRKM rate result is shown in Fig. 4b as a function of internal energy. As decreasing energy in the metastable window, relative abundance of the D loss diminishes rapidly, and eventually only the H loss occurs at low energy region. Apparently, this is due to the difference between the activation energies for the H and D loss as mentioned above. Considering all the contributions from the ions within the metastable window, the measured kinetic isotope effect can be extremely large as 500:1, of which exact value depends on detailed experimental conditions. Fig. 4b predicts that the isotope effect will be smaller than ∼10 if measured at higher energy than the metastable window.

3.2.2. *Intermolecular isotope effect on the water loss*

The isotope effect on water loss was demonstrated by Bowen et al. [9] from data on $CH_3CH_2CH_2OH^{\bullet+}$ and $CD_3CH_2CH_2OH^{\bullet+}$. According to their experiment, abundance ratio of H_2O and H loss is 97.4:2.6 in the matastable dissociation of $CH_3CH_2CH_2OH^{\bullet+}$. In the dissociation of $CD_3CH_2CH_2OH^{\bullet+}$, abundance ratio of HOD and H loss is 41.0:59.0. They estimated the isotope effect, k_{H_2O}:k_{HOD}, as 54:1 by normalizing these two ratios to the H loss abundances. To understand this isotope effect, we calculated $k_{isom}(E)$ ($=k_{H_2O}(E)$) and $k_H(E)$ for $CH_3CH_2CH_2OH^{\bullet+}$, and $k_{isom}(E)$ ($= k_{HOD}(E)$) and $k_H(E)$ for $CD_3CH_2CH_2OH^{\bullet+}$. The result is shown in Fig. 5 together with the calculated branching ratios, k_{H_2O}/k_H and k_{HOD}/k_H. The metastable window for dissociation of $CH_3CH_2CH_2OH^{\bullet+}$ is 89–102 kJ mol^{-1} as marked in the figure. Considering all the contributions from the dissociations occurring within the window, the abundance ratio of H_2O and H loss obtained experimentally is reasonable. The metastable window (94–108 kJ mol^{-1}) for dissociation of $CD_3CH_2CH_2OH^{\bullet+}$, however, moves to higher energy. The experimental ratio of HOD and H loss are also reasonably explained by the present rate-energy dependences.

Table 1
Relative energies in kJ mol^{-1} of $C_3H_8O^{\bullet+}$ ions, transition states, and fragment ions

Species	DFT[a]	MP2[b]	G2[c]	Exp $\Delta_f H^\circ_{0K}$[d]
$CH_3CH_2CH_2OH^{\bullet+}$ (*gauche*), **1g**	0.0	0	0	703[e] (0)
$CH_3CH_2CH_2OH^{\bullet+}$ (*gauche*), **1g′**	1.4			
$CH_3CH_2CH_2OH^{\bullet+}$ (*trans*), **1t**	0.04			
$^{\bullet}CH_2CH_2CH_2OH_2^+$, **2a**	12.4	−22	−18	714[f](11)
$^{\bullet}CH_2CH_2CH_2OH_2^+$, **2b**	10.1			
c-$C_3H_6^{\bullet+}\cdots H_2O$, **3a**	16.3			
c-$C_3H_6^{\bullet+}\cdots H_2O$, **3b**	19.4	8		
TS1gt	6.0			
TS1gg′	10.0			
TS1g′t	7.1			
TSH1g (H1 loss from **1g**)	91.3	74		802[g](99)
TSH2g (H2 loss from **2g**)	94.7			
TSH1g′ (H1 loss from **1g′**)	93.0			
TSH2g′ (H2 loss from **1g′**)	91.0			
TSH1a (H1 loss from **1t**)	93.2			
TSH2a (H2 loss from **1t**)	94.7			
TS12	72.8	104	76	795[g](92)
TS2ab	19.3			
TS23	37.2			
TS3ab	25.4			
$CH_3CH_2CHOH^+ + H^{\bullet}$ (H1 loss from **1g**)	86.6	45	55	781[h](78)
$CH_3CH_2CHOH^+ + H^{\bullet}$ (H2 loss from **1g**)	93.0			
$CH_3CH_2CHOH^+ + H^{\bullet}$ (H1 loss from **1g′**)	91.3			
$CH_3CH_2CHOH^+ + H^{\bullet}$ (H2 loss from **1g′**)	86.0			
$CH_3CH_2CHOH^+ + H^{\bullet}$ (H1 loss from **1t**)	91.3			
$CH_3CH_2CHOH^+ + H^{\bullet}$ (H2 loss from **1t**)	93.0			
c-$C_3H_6^{\bullet+} + H_2O$	61.1	71	50	782[i](79)

[a] Present result calculated at the UB3LYP/aug-cc-pVQZ//UB3LYP/6-31 + G(d) level of theory. The ZPEs calculated at the UB3LYP/6-31 + G(d) basis set were included. The calculated total energy and ZPE of **1g** are −194.0958106 and 0.106061 hartrees, respectively.
[b] MP2/6-31G(d, p) calculations from [10].
[c] G2(MP2, SVP) calculations from [12].
[d] Experimental 0 K heats of formation. The values in parentheses are the relative energies referred to **1**.
[e] From [11].
[f] From [2].
[g] From [1].
[h] From [10].
[i] From [21].

Then, why is the isotope effect estimated by Bowen et al. so large? They combined two abundance ratios to deduce the isotope effect on the water loss. There are two underlying assumptions in such an estimate. One is that the secondary isotope effect on H loss is neglected. Under this assumption, the ratios were normalized to the H loss abundances. To investigate the validity of the assumption, we calculated the intermolecular secondary isotope effects on H loss from $CH_3CH_2CH_2OH^{\bullet+}$ and $CD_3CH_2CH_2OH^{\bullet+}$ from their rate-energy dependences (Fig. 5c). The figure shows that the assumption is roughly valid near and above the ion internal energy 98 kJ mol^{-1}, but k_H for $CH_3CH_2CH_2OH^{\bullet+}$ is far smaller than k_H for $CD_3CH_2CH_2OH^{\bullet+}$ at internal energies below 98 kJ mol^{-1} where metastable dissociations occur. The second assumption is that metastable dissociations of the two isotopomers occur with the identical internal energy distributions. This is not true also since the metastable windows are different as shown in Fig. 5. The dissociation kinetics within the two metastable windows is significantly different. We conclude that invalidity of both the two assumptions would lead to the large intermolecular isotope effect on the water loss.

To obtain accurate isotope effects on water loss, experiments should be carried out for the molecular ions with well-defined energy. This has been performed using PEPICO

Table 2
Selected activation energies (in kJ mol^{-1}) used in RRKM rate calculations[a]

Reactions	E_0[b]
$CD_3CH_2CD(1)H(2)OH^{\bullet+}$ (**1g′**) → $^{\bullet}CD_2CH_2CDOHD^+$ (**2a**)	94.6
$CD_3CH_2CD(1)H(2)OH^{\bullet+}$ (**1g′**) → $CD_3CH_2CDOH^+ + H2^{\bullet}$	97.4
$CD_3CH_2CH(1)D(2)OH^{\bullet+}$ (**1g′**) → $CD_3CH_2CHOH^+ + D2^{\bullet}$	104.9
$CH_3CH_2CH_2OH^{\bullet+}$ (**1g**) → $^{\bullet}CH_2CH_2CH_2OH_2^+$ (**2a**)	91.6
$CH_3CH_2CH_2OH^{\bullet+}$ (**1g′**) → $CH_3CH_2CHOH^+ + H2^{\bullet}$	98.5
$CD_3CH_2CH_2OH^{\bullet+}$ (**1g**) → $^{\bullet}CD_2CH_2CH_2OHD^+$ (**2a**)	94.9
$CD_3CH_2CH_2OH^{\bullet+}$ (**1g′**) → $CD_3CH_2CHOH^+ + H2^{\bullet}$	97.3

[a] For H or D loss, the channels with the lowest barrier are listed.
[b] Referred to the energy of **1g**. For water or hydrogen atom loss, 19.8 or 7.5 kJ mol^{-1} was added, respectively, to the corresponding TS energies obtained by the UB3LYP/aug-cc-pVQZ//UB3LYP/6-31 + G(d) calculations. See text for details.

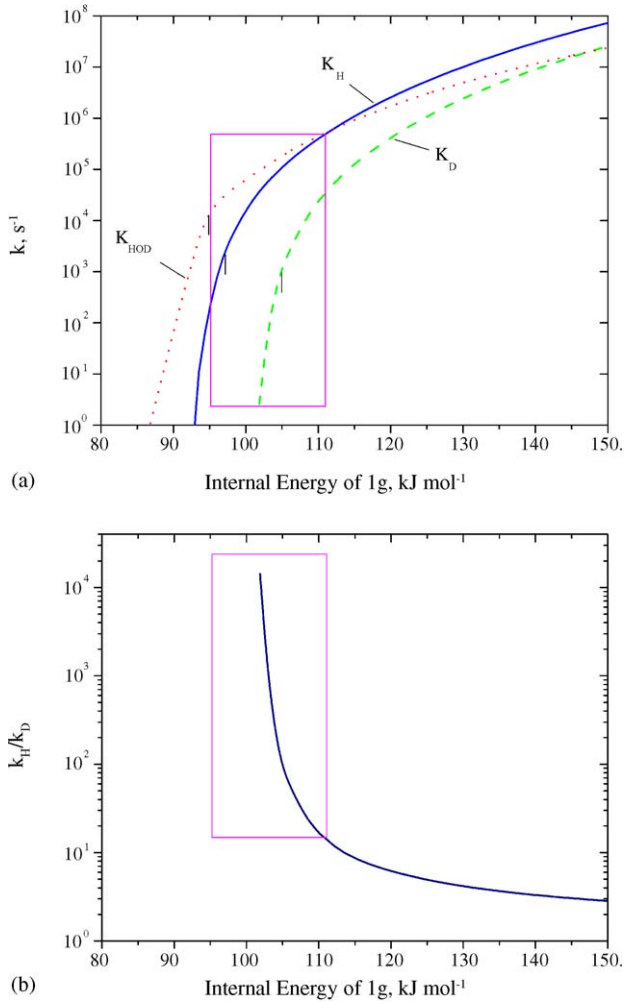

Fig. 4. (a) RRKM rate-energy dependences for HOD, H, and D loss from $CD_3CH_2CHDOH^{\bullet+}$. (b) The k_H/k_D ratio calculated from the RRKM rate-energy dependences. The metastable window ($k_{tot} = 10^4$–$10^6\ s^{-1}$) is marked as rectangles. Vertical bars represent the activation energies.

by Booze and Baer [11]. They reported $k_{H_2O}(E)$ and $k_{HOD}(E)$ for the dissociation of $CH_3CH_2CH_2OH^{\bullet+}$ and $CD_3CH_2CH_2OH^{\bullet+}$, respectively, which are similar to those in Fig. 5a. Their experimental results show normal isotope effects on the water loss. For example, at the ion internal energy of ~100 kJ mol^{-1} the k_{H_2O}:k_{HOD} ratio is estimated to be ~7. There exists another experimental evidence of the normal isotope effect on the water loss. Bowen et al. reported the collision-induced dissociation (CID) spectral data in their earlier study [8]. The abundance ratio of H_2O and H loss from $CH_3CH_2CH_2OH^{\bullet+}$ is 168:170, and that of HOD and H loss from $CD_3CH_2CH_2OH^{\bullet+}$ is 77:348. Ignoring the unimolecular contributions contained in the CID peaks, the k_{H_2O}:k_{HOD} isotope effect is estimated as 4.5 by the same method as above. This indicates that the two assumptions described above are more valid in the CID experiment than the metastable ion experiment. It is predicted that the molecular ions undergoing CID would have internal energy about 120 kJ mol^{-1} on the average by comparing the above exper-

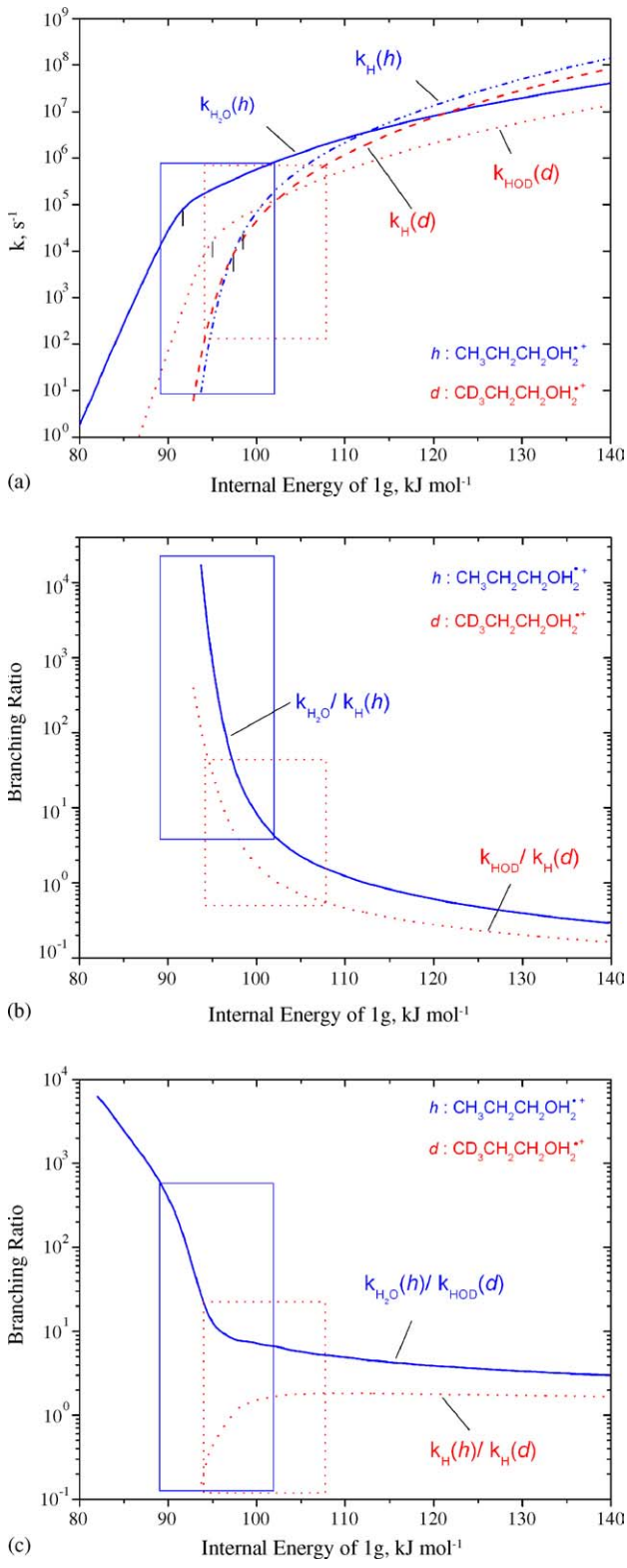

Fig. 5. (a) RRKM rate-energy dependences for H_2O and H loss from $CH_3CH_2CH_2OH^{\bullet+}$, and HOD and H loss from $CD_3CH_2CH_2OH^{\bullet+}$. (b) The intramolecular$k_{H_2O}/k_H$ and k_{HOD}/k_H ratios, and (c) the intermolecular k_{H_2O}/k_{HOD} and k_H/k_H ratios calculated from the RRKM rate-energy dependences. The metastable windows ($k_{tot} = 10^4$–$10^6\ s^{-1}$) are marked as solid and dotted rectangles for $CH_3CH_2CH_2OH^{\bullet+}$ and $CD_3CH_2CH_2OH^{\bullet+}$, respectively. Vertical bars represent the activation energies.

imental branching ratios to those calculated in the present work. Fig. 5c predicts, however, that the k_{H_2O}:k_{HOD} isotope effect can be very large if measured at a well-defined identical energy below 95 kJ mol^{-1} corresponding to the activation energy for the HOD loss. Whether one considers tunneling through the first isomerization barrier for the HOD loss affects the predicted isotope effect. Without considering the tunneling, the HOD loss would not occur at all below the activation energy, and then the isotope effect would go to infinite.

4. Conclusions

The pathway for water and hydrogen atom loss from *n*-propanol cation has been obtained by the DFT calculations. The water loss occurs via several isomerizations to distonic ions and ion-molecule complexes. The barrier for the isomerization **1g** → **2a** is the highest in the pathway for water loss. The isomerization barrier is lower than the barrier for H loss, agreeing with the experimental observations. The quantitative disagreement in energetic data, however, needs further improved theoretical investigations. The statistical RRKM calculations based on the DFT results predict the large kinetic deuterium isotope effects on the water and hydrogen atom loss reported previously by metastable ion studies. Near activation barriers, intramolecular k_H/k_D isotopic effects can be extremely large because metastable window can contain the energy region where the metastable ion does not undergo D loss at all, but do H loss, as in the case of H and D loss from $CD_3CH_2CHDOH^{\bullet+}$. In investigating intermolecular isotope effects on metastable ion dissociations, one should bear in mind that the molecular ions sampled in the dissociations can have different internal energy distributions.

Acknowledgement

This work was supported by the Korea Research Foundation Grant (KRF-2004-041-C00169).

References

[1] K.M.A. Refaey, W.A. Chupka, J. Chem. Phys. 48 (1968) 5205.
[2] J.L. Holmes, A.A. Mommers, J.E. Szulejko, J.K. Terlouw, J. Chem. Soc. Chem. Commun. (1984) 165.
[3] C. Wesdemiotis, P.O. Danis, R. Feng, J. Tso, F.W. McLafferty, J. Am. Chem. Soc. 107 (1985) 8059.
[4] M. Yamamoto, T. Takeuchi, K. Nishimoto, Int. J. Mass Spectrom. Ion Phys. 46 (1983) 239.
[5] T. Takeuchi, S. Ueno, M. Yamamoto, T. Matsushita, K. Nishimoto, Int. J. Mass Spectrom. Ion Process. 64 (1985) 33.
[6] J.D. Shao, T. Baer, J.C. Morrow, M.L. Fraser-Monteiro, J. Chem. Phys. 87 (1987) 5242.
[7] D.J. McAdoo, M.S. Ahmed, C.E. Hudson, Int. J. Mass Spectrom. Ion Process. 100 (1990) 579.
[8] R.D. Bowen, A.W. Colburn, P.J. Derrick, J. Am. Chem. Soc. 113 (1991) 1132.
[9] R.D. Bowen, S.J. Mandeville, M.A. Trikoupis, J.K. Terlouw, Chem. Commun. (1999) 2111.
[10] J.A. Booze, T. Baer, J. Phys. Chem. 96 (1992) 5710.
[11] J.A. Booze, T. Baer, J. Phys. Chem. 96 (1992) 5715.
[12] G. Bouchoux, N. Choret, Int. J. Mass Spectrom. 201 (2000) 161.
[13] T. Baer, W.L. Hase, Unimolecular Reaction Dynamics: Theory and Experiments, Oxford, New York, 1996.
[14] M.J. Frisch, G.W. Trucks, H.B. Schlegel, G.E. Scuseria, M.A. Robb, J.R. Cheeseman, J.A. Montgomery Jr., T. Vreven, K.N. Kudin, J.C. Burant, J.M. Millam, S.S. Iyengar, J. Tomasi, V. Barone, B. Mennucci, M. Cossi, G. Scalmani, N. Rega, G.A. Petersson, H. Nakatsuji, M. Hada, M. Ehara, K. Toyota, R. Fukuda, J. Hasegawa, M. Ishida, T. Nakajima, Y. Honda, O. Kitao, H. Nakai, M. Klene, X. Li, J.E. Knox, H.P. Hratchian, J.B. Cross, C. Adamo, J. Jaramillo, R. Gomperts, R.E. Stratmann, O. Yazyev, A.J. Austin, R. Cammi, C. Pomelli, J.W. Ochterski, P.Y. Ayala, K. Morokuma, G.A. Voth, P. Salvador, J.J. Dannenberg, V.G. Zakrzewski, S. Dapprich, A.D. Daniels, M.C. Strain, O. Farkas, D.K. Malick, A.D. Rabuck, K. Raghavachari, J.B. Foresman, J.V. Ortiz, Q. Cui, A.G. Baboul, S. Clifford, J. Cioslowski, B.B. Stefanov, G. Liu, A. Liashenko, P. Piskorz, I. Komaromi, R.L. Martin, D.J. Fox, T. Keith, M.A. Al-Laham, C.Y. Peng, A. Nanayakkara, M. Challacombe, P.M.W. Gill, B. Johnson, W. Chen, M.W. Wong, C. Gonzalez, J.A. Pople, Gaussian 03 (Revision B.04), Gaussian, Inc., Pittsburgh, PA, 2003.
[15] (a) A.D. Becke, J. Chem. Phys. 98 (1993) 5648;
(b) C. Lee, W. Yang, R.G. Parr, Phys. Rev. B 37 (1988) 785;
(c) P.J. Stevens, F.J. Devlin, C.F. Chablowski, M.J. Frisch, J. Phys. Chem. 98 (1994) 11623.
[16] (a) P. Hohenberg, W. Kohn, Phys. Rev. 136 (1964) 864B;
(b) W. Kohn, L.J. Sham, Phys. Rev. 140 (1965) 1133A;
(c) J.A. Pople, P.M.W. Gill, B.G. Johnson, Chem. Phys. Lett. 199 (1992) 557.
[17] (a) J. Noga, R.J. Bartlett, J. Chem. Phys. 86 (1987) 7041;
(b) K. Ragavachari, G.W. Trucks, J.A. Pople, M. Head-Gordon, Chem. Phys. Lett. 157 (1989) 479;
(c) R.J. Barett, J.D. Watts, S.A. Kucharski, J. Noga, Chem. Phys. Lett. 165 (1990) 513.
[18] C. Eckart, Phys. Rev. 35 (1930) 1303.
[19] D.J. Bellville, N.L. Bauld, J. Am. Chem. Soc. 104 (1982) 5700.
[20] J.W. Gauld, L. Radom, Chem. Phys. Lett. 275 (1997) 28.
[21] S.G. Lias, J.E. Bartmass, J.F. Liebman, J.L. Holmes, R.D. Levine, W.G. Mallard, J. Phys. Chem. Ref. Data 17 (Suppl. 1) (1988).
[22] R.G. Cooks, J.H. Beynon, R.M. Caprioli, G.R. Lester, Metastable Ions, Elsevier, Amsterdam, 1973.